Geochimica et Cosmochimica Acta, Vol. 69, No. 24, pp. 5819–5830, 2005

0016-7037/05 $30.00 + .00

doi:10.1016/j.gca.2005.08.007

Constraints on the U-Pb isotopic systematics of Mars inferred from a combined U-Pb, Rb-Sr, and Sm-Nd isotopic study of the Martian meteorite Zagami

Lars E. Borg,[1,*] Jennifer E. Edmunson,[1] and Yemane Asmerom[2]

[1]Institute of Meteoritics, University of New Mexico, Albuquerque, New Mexico 87131, USA
[2]Department of Earth and Planetary Sciences, University of New Mexico, Albuquerque, New Mexico 87131, USA

(*Received March* 22, 2005; *accepted in revised form August* 5, 2005)

Abstract—Uranium-lead, Rb-Sr, and Sm-Nd isotopic analyses have been performed on the same whole-rock, mineral, and leachate fractions of the basaltic martian meteorite Zagami to better constrain the U-Pb isotopic systematics of martian materials. Although the Rb-Sr and Sm-Nd systems define concordant crystallization ages of 166 ± 6 Ma and 166 ± 12 Ma, respectively, the U-Pb isotopic system is disturbed. Nevertheless, an age of 156 ± 6 Ma is derived from the ^{238}U-^{206}Pb isotopic system from the purest mineral fractions (maskelynite and pyroxene). The concordance of these three ages suggest that the ^{238}U-^{206}Pb systematics of the purest Zagami mineral fractions have been minimally disturbed by alteration and impact processes, and can therefore be used to constrain the behavior of U and Pb in the Zagami source region. The μ value of the Zagami source region can be estimated, with some confidence from the ^{238}U-^{206}Pb isochron, to be 3.96 ± 0.02. Disturbance of the U-Pb isotopic systems means that this represents a minimum value. The μ value of the Zagami source is significantly lower than the μ values estimated for most basaltic magma sources from Earth and the Moon. This is surprising given the high initial ^{87}Sr/^{86}Sr ratio (0.721566 ± 82) and low initial ε_{Nd} value (−7.23 ± 0.17) determined for Zagami that indicate that this sample is derived from one of the most highly fractionated reservoirs from any known planetary body. This suggests that Mars is characterized by a low bulk planet U/Pb ratio, a feature that is consistent with its relatively volatile-rich nature.

The leachates contain terrestrial common Pb that was probably added to the meteorite during handling, curation, or sawing. The mineral fractions, particularly those with significant amounts of impact melt glass, contain a second contaminant. The presence of this contaminant results in Pb-Pb ages that are older than the crystallization age of Zagami, indicating that the contaminant is characterized by a high ^{207}Pb/^{206}Pb ratio. Such a contaminant could be produced by removal of single-stage Pb from a relatively high μ martian reservoir before ~1.8 Ga, and therefore could be an ancient manifestation of hydrous alteration of martian surface material.

1. INTRODUCTION

The uranium-lead isotopic system provides powerful insights into both the timing of events occurring on planetary bodies and the geochemical behavior of U and Pb within planetary environments (e.g., Chen and Wasserburg, 1986a; Premo and Tatsumoto 1991; Borg et al., 1999). Although the timing of many events can often be gleaned from other isotopic systems such as K-Ar, Rb-Sr, and Sm-Nd, understanding the geochemical behavior of U and Pb in martian mantle and crustal reservoirs requires U-Pb isotopic analysis. Uranium-lead isotopic analysis can be used to constrain the relative abundances of these elements within a given planet, offer insights into how these elements are partitioned during planetary differentiation and magma production, and record how these elements are mobilized and redistributed on planetary surfaces. Despite its potential usefulness, the application of U-Pb chronology to samples from relatively large differentiated bodies is often hampered by the ease at which this system is disturbed by impact metamorphism, secondary alteration, and terrestrial contamination. As a result, the interpretation of U-Pb isotopic data from the Moon and Mars is seldom unambiguous unless additional constraints on the age of the sample, and/or differentiation history of the planet, can be obtained from alternative sources (e.g., Unruh and Tatsumoto, 1977; Premo and Tatsumoto, 1991).

Here we present U-Pb, Rb-Sr, and Sm-Nd isotopic measurements completed on the same whole rocks, mineral fractions, and leachates from the basaltic martian meteorite Zagami. The goal of this study is to better understand the geochemical processes that influence the behavior of the U-Pb isotopic systematics on Mars by interpreting the U-Pb isotopic data in the context of the Rb-Sr and Sm-Nd crystallization ages of Zagami and in the context of the differentiation history of this planet. Although the disturbed nature of the U-Pb isotopic systematics preclude the derivation of clear age determinations from this system, the interpretation of the U-Pb data in the context of Rb-Sr and Sm-Nd crystallization ages helps define the nature of these disturbances, the composition and evolutionary history of Pb contamination in Zagami, and the initial Pb isotopic composition of the Zagami source region.

2. GEOCHEMICAL EVOLUTION OF MARS

The objective of this study is to constrain the geochemical evolution of Pb on Mars through U-Pb, Rb-Sr, and Sm-Nd isotopic analyses of the same mineral fractions derived from the basaltic meteorite Zagami. This is accomplished by dissecting this meteorite using detailed mineral separation procedures that permit the nature and extent of U-Pb isotopic disequilib-

* Author to whom correspondence should be addressed (lborg@unm.edu).

rium to be better understood. To better interpret the U-Pb isotopic systematics of Zagami, it is necessary to review a few of the fundamental geochemical and isotopic systematics observed in the martian meteorite suite. These systematics provide a critical framework in which to interpret the new U-Pb isotopic data. The most germane issues in this regard are how the Rb-Sr and Sm-Nd isotopic systematics of the martian meteorite suite constrain (1) the extent and timing of planetary differentiation and (2) the relationship of Zagami to the other basaltic shergottites.

2.1. Extent and Timing of Planetary Differentiation

The martian meteorite suite displays an extreme range of geochemical and isotopic compositions. For example, chondrite-normalized REE patterns of bulk shergottites vary from almost flat ($^{147}Sm/^{144}Nd = 0.18$) to strongly light-rare-earth-element (LREE)-depleted ($^{147}Sm/^{144}Nd = 0.50$). There is also a very large range of initial $^{87}Sr/^{86}Sr$ ratios (0.701 to 0.726) and ε_{Nd}^{143} values (-8 to $+46$; Shih et al., 1982; Borg et al., 1997) forming a compositional continuum. One end of the continuum is represented by meteorites with trace element and isotopic compositions indicative of derivation from a highly depleted source region, whereas the other end of the continuum is represented by meteorites that appear to be derived from more evolved source regions that are more enriched in incompatible elements. These observations have been interpreted to reflect mixing of sources produced by an early martian planetary-scale differentiation event (e.g., Jones, 1989; Borg et al., 1997; Nyquist et al., 2001; Borg and Draper, 2003; Borg et al., 2003).

The presence of nonchondritic abundances of decay products of short-lived isotopic systems such as ^{142}Nd and ^{182}W have been observed in the martian sample suite (Harper et al., 1995; Borg et al., 1997; Lee and Halliday, 1997; Kleine et al., 2004; Foley et al., 2005), and suggest that core formation and silicate differentiation occurred early in the history of the planet. Borg et al. (1997, 2003) have argued that the $\varepsilon_{Nd}^{143} - \varepsilon_{Nd}^{142}$ systematics are consistent with a two-stage model of silicate differentiation for martian basalt source regions. This model is consistent with martian silicate differentiation occurring ~30 Ma after planetary formation. The fact that isotopic anomalies in short-lived decay systems are present in relatively young rocks with ages of 165 to 1300 Ma (Nyquist et al. 2001; Borg and Drake, 2005) further indicates that the basalt source regions have remained isolated (unmixed) since the time they formed. Thus, Mars appears to have undergone early differentiation in which highly fractionated reservoirs formed and remained isolated from one another until fairly recently.

2.2. Relationship of Zagami to the Other Basaltic Meteorites

Zagami is a basaltic shergottite composed primarily of pyroxenes (70%–80%) and maskelynite (10%–25%), with 2 to 4% mesostasis, 2 to 3% oxides, 0.5 to 1.3% phosphates, 0.1 to 0.9% impact melt glass, and 0.2 to 0.6% sulfides (Stolper and McSween, 1979; McCoy et al., 1992). It has a cumulate texture, typical of the shergottites, and is composed of at least three distinct lithologies (McCoy et al., 1992). The two most voluminous lithologies are distinguished on the basis of grain size.

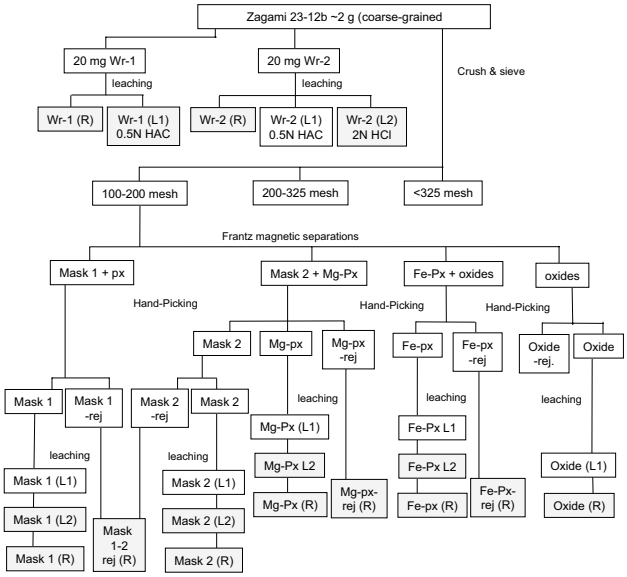

Fig. 1. Flow diagram illustrating the mineral separation procedure used for Zagami. Residues (R), 2 N HCl leachates (L2), and 0.5 M acetic acid leachate (L1) in light gray have been analyzed for U-Pb, Rb-Sr, and Sm-Nd.

The coarse lithology is composed of grains with an average size of 0.36 mm, whereas the fine-grained lithology contains grains that have an average size of 0.24 mm. Zagami has relatively high incompatible element abundances and a relatively light rare earth element enriched pattern. Thus, it is compositionally and mineralogically similar to the basaltic shergottites Shergotty and Los Angeles. Whole-rock Sr and Nd isotopic compositions of these three meteorites are also very similar (Shih et al., 1982; Nyquist et al., 1995; Nyquist et al., 2000). Therefore, although Zagami is mineralogically and texturally akin to many basaltic meteorites, it has incompatible element abundances and isotopic systematics typical of those meteorites that are derived from the most geochemically evolved reservoirs.

3. ANALYTICAL TECHNIQUES

A 2 g sample of the coarse-grained Zagami lithology was allocated from the meteorite collection at the University of New Mexico. This sample was adjacent to the sample allocated to L. Nyquist for isotopic analyses, making the Rb-Sr and Sm-Nd results of this study directly comparable to those of Nyquist et al. (1995). The unfractured chip was first sonicated in 4x quartz-distilled water for 10 min. The sample was then crushed in a sapphire mortar and pestle and a whole-rock chip was removed. The remainder of the sample was sieved at 100, 200, and 325 mesh. The mineral separation procedure is summarized in Figure 1. First, the 100 to 200 mesh fraction was run through a Frantz isodynamic separator yielding fractions rich in maskelynite (Mask), Mg-pyroxene (Mg-Px), Fe-pyroxene (Fe-Px), and oxides (Ox). Then, these fractions were handpicked to estimated purities of >99%. The primary impurities observed in the mineral fractions were other igneous minerals or impact melt glasses. Isotopic analyses were also completed on the leached residues of material rejected by the handpicking process, that is, Mask 1–2 rej (R), Fe-Px rej (R), and Mg-Px rej (R) that contained grains composed of compound minerals and contained large amounts of impact melt glass.

The mineral, reject, and whole-rock fractions were leached in a sonicator in 0.5 M acetic acid (leachates designated L1) and 1N HCl (leachates designated L2) for 10 min each. The residues (R) were then

Table 1. Zagami Rb-Sr isotopic data.

Fraction	Wt (mg)	Rb (ppm)	Rb (ng)	Sr (ppm)	Sr (ng)	$\frac{^{87}Rb}{^{86}Sr}$ [a]	$\frac{^{87}Sr}{^{86}Sr}$ [b]
Wr 1 (R)	24.66	6.61	163	29.21	720	0.6548 ± 66	0.723069 ± 10
Wr 2 (R)	14.44	7.52	109	36.74	531	0.5922 ± 59	0.722963 ± 10
Wr 2 (L2)			1.7		52.1	0.09612 ± 96	0.721633 ± 10
Mask 1 (R)	1.29	2.38	3.1	210.3	271	0.03280 ± 33	0.721637 ± 10
Mask 1 (L2)			0.13		9.0	0.04098 ± 97	0.721478 ± 19
Mask 2 (R)	23.64	8.34	197	177.6	4198	0.1359 ± 14	0.721977 ± 10
Mask 2 (L2)			0.6		90.1	0.01851 ± 19	0.721624 ± 10
Mg-Px (R)	33.16	1.34	44.6	3.71	123	0.937 ± 94	0.723995 ± 10
Mg-Px (L2)			0.18		10.1	0.05174 ± 86	0.720915 ± 27
Fe-Px (R)	70.53	2.67	188	4.27	298	1.810 ± 18	0.726028 ± 10
Fe-Px (L2)			0.6		62.9	0.02621 ± 26	0.721384 ± 10
Ox (R)	14.55	9.41	137	27.63	402	0.9848 ± 99	0.723908 ± 12
Mask 1–2 rej (R)	16.46	60.5	995	157.5	2592	1.117 ± 11	0.724159 ± 10
Mg-Px rej (R)	67.48	8.30	560	20.94	1413	1.147 ± 15	0.724178 ± 10
Fe-Px rej (R)	33.38	8.18	273	14.52	485	1.630 ± 16	0.725326 ± 10
NBS-987 (N = 7)							0.710244 ± 14[c]

$^{85}Rb/^{87}Rb$ ratio of six runs of the NBS-984 Rb standard = 2.624 ± 20 ($2\sigma_p$).

Isochrons are calculated using either $2\sigma_p$ (from standard runs) or $2\sigma_m$ (from measured isotopic ratios), whichever is larger.

Wr = whole rock; Px = pyroxene; Mask = maskelynite; Ox = oxide; L2 = HCl leachate; R = residue; rej = portion of mineral fraction rejected after handpicking.

[a] Error limits apply to last digits and include a minimum uncertainty of 1% plus 50% of the blank correction for Rb and Sr added quadratically.

[b] Normalized to $^{86}Sr/^{88}Sr = 0.1194$. Uncertainties refer to last digits and are $2\sigma_m$ calculated from the measured isotopic ratios. $2\sigma_m = [\Sigma(m_i - \mu)^2/(n(n-1))]^{1/2}$ for n ratio measurements m_i with mean value m.

[c] Uncertainties refer to last digits and are $2\sigma_p$. $2\sigma_p = [\Sigma(M_i - \pi)^2/(N-1)]^{1/2}$ for N measurements M_i with mean value π.

digested using a combination of hydrofluoric, nitric, and hydrochloric acids. Isotope dilution techniques were preformed on (~5%) aliquots of the digested samples to determine the concentrations of Sr and Nd in the samples and to ensure proper spike/sample ratios. The remaining ~95% aliquots were spiked with mixed ^{233}U-^{236}U-^{205}Pb, ^{87}Rb-^{84}Sr, and ^{149}Sm-^{150}Nd isotopic tracers. To minimize Pb contamination, the Rb-Sr and Sm-Nd isotopic tracers were prepared from stock solutions after Pb was removed using ion exchange techniques. Uranium-lead, Rb-Sr, and Sm-Nd were sequentially separated from the same solutions. Uranium-lead was separated using 100 to 250 μL anion resin columns in HCl and HBr. Rubidium-strontium and REE were separated from the anion chemistry washes using cation exchange columns in 2N and 6N HCl. The REE were purified using RE-spec resin in 0.05N and 1N HNO_3 before loading on pressurized 2-hydroxyisobutyric acid columns. The 2-hydroxyisobutyric acid was separated from the Sm and Nd using 2 mL cation clean-up columns. Total procedural blanks (N = 2–4) include contributions associated with the tracers and were U = 4 ± 3 pg, Pb = 22 ± 6 pg, Rb = 6 ± 4 pg, Sr = 11 ± 4 pg, Sm = 5 ± 3 pg, and Nd = 9 ± 3 pg (1 sigma).

Isotopic measurements were done in the Radiogenic Isotope Laboratory at the University of New Mexico on a Micromass (VG) Sector 54 mass spectrometer. This mass spectrometer has seven Faraday cups and an ion counting Daly with a dark noise of 0.1 counts per second. It has a high-abundance sensitivity wide aperture retarding potential (WARP) filter between the axial cup and Daly multiplier. Uranium was loaded with graphite and run as a metal. The mixed ^{233}U-^{236}U spike was used to correct for mass fractionation. Large Pb samples were run using the Faraday cups for all masses except ^{205}Pb, which was run simultaneously on the Daly ion counter. Typical precision on $^{205}Pb/^{204}Pb$ ratios in this configuration is 0.01 to 0.05%. A dynamic routine using the Daly to count both ^{205}Pb and ^{204}Pb was used for smaller samples. Faraday-Daly relative gains were routinely run before and after each Pb analysis. Mass fractionation of Pb on the mass spectrometer was determined to be 0.10 ± 0.02% per atomic mass unit based on replicate analyses of NBS-981 Pb standard. Rubidium was run on oxidized Ta filaments. Mass fractionation of Rb was determined to be 0.6 ± 0.1% based on replicate analyses of the NBS-984 Rb standard. Sr was loaded in H_3PO_4 and Ta_2O_5 on Re filaments and was normalized to $^{86}Sr/^{88}Sr = 0.1194$. Measured $^{87}Sr/^{86}Sr$ ratios were normalized to the NBS-987 standard value of 0.710250. Neodymium and Sm were run as oxides on single Re filaments using an oxygen bleed system at 5×10^{-6} torr. Mass fractionation of Nd was corrected using $^{146}Nd/^{144}Nd = 0.7219$, whereas Sm was corrected using $^{147}Sm/^{152}Sm = 0.560828$. Measured $^{143}Nd/^{144}Nd$ ratios were normalized to the LaJolla Nd standard value of 0.511850. Results of Sr and Nd standard runs are compiled in Tables 1 and 2.

4. RB-SR AND SM-ND ISOTOPIC SYSTEMATICS

The results of Rb-Sr, Sm-Nd, and U-Pb isotopic analyses are presented in Tables 1, 2, and 3. The Rb-Sr and Sm-Nd isotopic data are discussed first because they constrain the crystallization age of Zagami, providing a basis in which to interpret the U-Pb data. The ages presented below are calculated using Isoplot/Ex v. 2.49 (Ludwig, 2001).

4.1. Rb-Sr Isochron

Figure 2 is a Rb-Sr isochron diagram of Zagami whole rocks, mineral fractions, and leachates analyzed in this study. The purest mineral fractions, Mask 1 (R), Mg-Px (R), and Fe-Px (R), yield an age of 176 ± 2 Ma with an initial Sr isotopic composition of 0.721556 ± 22 and a mean square weighted derivative (MSWD) = 1.1. The low uncertainties and MSWD, in large part, reflect the small number of fractions used to define this age. As a consequence, the most representative age is probably defined by all of the mineral fractions. The silicate and oxide mineral and reject fractions define a Rb-Sr age of 166 ± 6 Ma and an initial $^{87}Sr/^{86}Sr$ ratio of 0.721566 ± 82 (MSWD = 17). The age and initial Sr isotopic composition of the coarse-grained Zagami lithology determined by Nyquist et al. (1995) and Shih et al. (1982) are 183 ± 6 Ma, 0.721604 ± 57 and 180 ± 4 Ma, 0.72145 ± 5, respectively, and are in good agreement with the results presented here for the same lithology. Our mineral fractions define a larger range of $^{87}Rb/^{86}Sr$ ratios and somewhat less scatter, most likely reflecting their greater purity. The maskelynite mineral fractions analyzed in

Table 2. Zagami Sm-Nd isotopic data.

Fraction	Wt (mg)	Sm (ppm)[a]	Sm (ng)	Nd (ppm)[a]	Nd (ng)	$\frac{^{147}Sm}{^{144}Nd}$ [a]	$\frac{^{143}Nd}{^{144}Nd}$ [b]
Wr 1 (R)	24.66	1.947	48.0	4.830	119	0.24374 ± 24	0.512311 ± 10
Wr 2 (R)	14.44	0.250	3.6	0.371	5.4	0.40665 ± 55	0.512489 ± 19
Wr 2 (L2)			1.6		42.7	0.23024 ± 23	0.512242 ± 10
Mask 1 (L2)			2.2		5.6	0.23325 ± 45	0.512168 ± 17
Mask 2 (R)	23.64	0.063	1.5	0.143	3.4	0.26468 ± 74	0.512351 ± 11
Mask 2 (L2)			41.7		110	0.22908 ± 50	0.512293 ± 10
Mg-Px (R)	33.16	0.316	10.5	0.468	15.5	0.40858 ± 41	0.512500 ± 10
Mg-Px (L2)			3.0		8.2	0.22058 ± 31	0.512294 ± 12
Fe-Px (R)	70.53	0.263	18.5	0.375	26.4	0.42338 ± 42	0.512499 ± 10
Fe-Px (L2)			23.3		62.3	0.22549 ± 23	0.512301 ± 10
Ox (R)	14.55	1.890	27.5	4.820	70.1	0.23706 ± 24	0.512320 ± 10
Mask 1–2 rej (R)	16.46	0.068	1.1	0.152	2.5	0.2700 ± 13	0.512354 ± 21
Mg-Px rej (R)	67.48	0.309	20.8	0.465	31.4	0.40165 ± 40	0.512494 ± 10
Fe-Px rej (R)	33.38	0.335	11.2	0.513	17.1	0.39490 ± 39	0.512503 ± 10
LaJolla Nd (N = 12)					2–10		0.511873 ± 17[c]

All samples and standards run as NdO^+.

Wr = whole rock; Px = pyroxene; Mask = maskelynite; Ox = oxide; L2 = HCl leachate; R = residue; rej = portion of mineral fraction rejected after handpicking.

[a] Error limits apply to last digits and include a minimum uncertainty of 0.5% plus 50% of the blank correction for Sm and Nd added quadratically.

[b] Normalized to $^{146}Nd/^{144}Nd = 0.7219$. Uncertainties refer to last digits and are $2\sigma_m$ calculated from the measured isotopic ratios. $2\sigma_m = [\Sigma(m_i - \mu)^2/(n(n-1))]^{1/2}$ for n ratio measurements m_i with mean value m.

[c] Error limits refer to last digits and are $2\sigma_p$. $2\sigma_p = [\Sigma(M_i - \pi)^2/(N-1)]^{1/2}$ for N measurements M_i with mean value π. Isochron are calculated using either $2\sigma_p$ (from standard runs) or $2\sigma_m$ (from measured isotopic ratios), whichever is larger.

this study have $^{87}Rb/^{86}Sr$ ratios near zero, and therefore place relatively tight limits on the initial Sr isotopic composition of Zagami. The Rb-Sr isotopic compositions of the L2 leachates were also determined. All but one of the leachates lie below the isochron defined by the silicate mineral fractions and whole rocks, indicating that they contain a relatively unradiogenic Sr component that is not indigenous to, that is, in isotopic equilibrium with, the Zagami silicate fractions.

It is important to note that deviations of mineral, whole-rock, and leachate fractions from individual Rb-Sr (and Sm-Nd; Fig. 3) isochrons are a ubiquitous feature of basaltic martian meteorites (e.g., Nyquist et al., 1979; Shih et al., 1982; Nyquist et al., 1995; Borg et al., 1997; Nyquist et al., 2000; Borg et al., 2002; Borg et al., 2003). This is a result of these samples having undergone varying degrees of thermal metamorphism associated with shock and having been subjected to alteration on Mars and Earth. Compared to most martian meteorites, however, Zagami demonstrates minimally disturbed isotopic systematics as demonstrated by Rb-Sr (and Sm-Nd) ages that are defined by all but a few of the analyzed fractions. Never-

Table 3. Zagami U-Pb isotopic data.

Fraction	Wt (mg)	U (ppm)	Pb (ppm)	^{238}U (pmol)	^{206}Pb (pmol)	$\frac{^{238}U}{^{204}Pb}$ [a]	$\frac{^{208}Pb}{^{204}Pb}$ [b]	$\frac{^{207}Pb}{^{204}Pb}$ [b]	$\frac{^{206}Pb}{^{204}Pb}$ [b]
Wr (R)	24.66	0.126	0.837	13.0	23.0	8.427 ± 38	35.075 ± 55	13.742 ± 17	14.937 ± 15
Wr (L1)				11.7	5.57	35.46 ± 15	36.829 ± 60	14.575 ± 20	16.899 ± 18
Mask 1 (R)	39.36	0.118	0.626	19.4	26.4	10.09 ± 8	33.693 ± 73	13.199 ± 17	13.515 ± 14
Mask 1 (L2)				2.89	1.23	43.0 ± 4.6	37.24 ± 22	15.010 ± 87	18.133 ± 99
Mask 2 (R)	23.64	0.405	1.30	39.9	32.8	16.54 ± 6	33.633 ± 49	13.182 ± 15	13.582 ± 10
Mask 2 (L2)				13.7	3.76	59.90 ± 48	36.673 ± 64	14.059 ± 23	16.384 ± 26
Mg-Px (R)	33.20	0.115	0.056	16.0	2.22	118.2 ± 5.9	35.11 ± 24	13.465 ± 99	16.234 ± 94
Mg-Px (L2)				2.86	1.88	28.1 ± 21	37.73 ± 13	15.161 ± 53	18.421 ± 58
Fe-Px (R)	70.53	0.140	0.117	41.3	9.33	65.98 ± 2.4	34.275 ± 57	13.423 ± 19	14.859 ± 15
Fe-Px (L2)				18.0	7.15	45.85 ± 4.4	39.48 ± 27	15.53 ± 12	18.21 ± 16
Ox (R)	14.55	7.69	0.920	467	16.1	474.3 ± 1.5	34.601 ± 62	13.633 ± 21	16.341 ± 21
Mask 1–2 rej (R)	16.46	1.87	4.16	128	74.3	23.86 ± 16	33.553 ± 55	13.156 ± 18	13.844 ± 14
Mg-Px rej (R)	67.48	0.148	0.379	41.7	27.3	20.59 ± 40	33.347 ± 82	13.128 ± 33	13.484 ± 33
Fe-Px rej (R)	33.38	0.179	0.456	25.0	16.4	21.08 ± 8	33.884 ± 56	13.300 ± 18	13.816 ± 16
NBS-981 (N = 17)[b]							36.505 ± 72	15.438 ± 21	16.985 ± 17

Wr = whole rock; Px = pyroxene; Mask = maskelynite; Ox = oxide; L1 = HAc leachate; L2 = HCl leachate; R = residue; rej = portion of mineral fraction rejected after handpicking. Reject samples leached in HCl.

[a] Error limits apply to last digits and include a minimum uncertainty of 0.5% plus 50% of the blank correction for U and Pb added quadratically.

[b] Values are weighted averages of N = 1–10 mass spectrometry runs. Error limits refer to last digits and include a minimum of 0.02% per annu for uncertainty of fractionation correction plus the weighted average of $2\sigma_p$ added quadratically. $2\sigma_p = [\Sigma(M_i - \pi)^2/(N-1)]^{1/2}$ for N measurements M_i with mean value π.

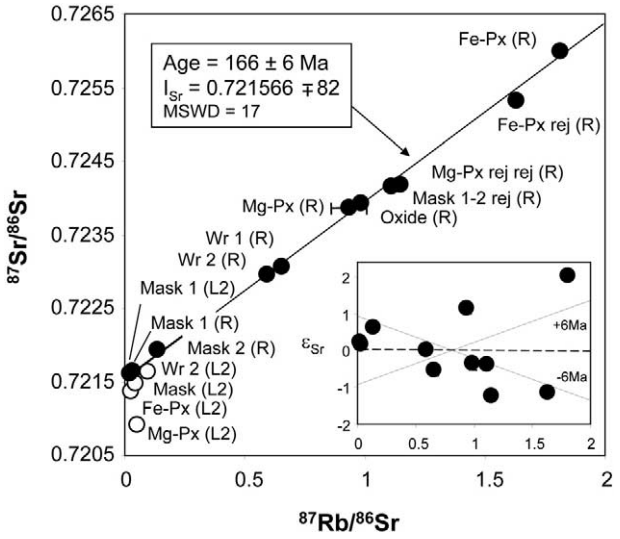

Fig. 2. Rb-Sr isochron plot of Zagami whole-rock, mineral, and leachate fractions. The purest mineral fractions, Mask 1 (R), Mg-Px (R), and Fe-Px (R) yield an age of 176 ± 2 Ma with an initial Sr isotopic composition of 0.721556 ± 22 and a MSWD = 1.1 The most representative age, defined by all of the silicate and oxide mineral and reject fractions (filled circles), is 166 ± 6 Ma and an initial $^{87}Sr/^{86}Sr$ ratio of 0.721566 ± 82 (MSWD = 17). Most leachates do not lie on the isochron (open circles). Inset represents deviation of individual fractions from the isochron, in epsilon units.

theless, it is the concordance between the Rb-Sr and Sm-Nd ages (discussed below) which indicates that the Rb-Sr age reflects the crystallization age of the sample.

Nyquist et al. (1995) completed Rb-Sr isotopic analyses on both the coarse and fine-grained portions of Zagami. They noted that the crystallization ages from the coarse and fine-grained fractions were within uncertainty of one another, but the initial Sr isotopic compositions were not. They interpreted this to reflect slightly different source regions for the parental magmas of the two lithologies. Note, however, that the variable presence of an unradiogenic leachable component in the coarse and fine-grained lithologies could account for the different initial Sr isotopic compositions of the two lithologies. To account for its higher initial Sr isotopic composition, the fine-grained lithology is expected to contain less of this component. Interestingly, the fine-grained mineral fractions analyzed by Nyquist et al. (1995) were leached in HCl, whereas the coarse-grained mineral fractions were not. The differences in the initial Sr isotopic compositions of the coarse and fine-grained lithologies could therefore reflect removal of an unradiogenic Sr component from the fine-grained mineral fractions by leaching.

The Zagami age and initial $^{87}Sr/^{86}Sr$ ratio are very similar to those determined for Shergotty (165 ± 8 Ma and 0.72260 ± 12; Nyquist et al., 1979) and Los Angeles (166 ± 11 Ma and 0.720997 ± 51; Nyquist et al., 2000). The initial $^{87}Sr/^{86}Sr$ ratio of these meteorites is significantly higher than the initial Sr isotopic compositions determined on all other martian meteorites, some of which have $^{87}Sr/^{86}Sr$ ratios as low as 0.7013 (Borg et al., 1997). If the Zagami source formed from a planet with the initial Sr isotopic composition of best achondrite basaltic initial (BABI $^{87}Sr/^{86}Sr$ = 0.69898) at 4.558 Ga, then the Zagami source is required to have a $^{87}Rb/^{86}Sr$ ratio of 0.356. In comparison, the source regions of terrestrial basalts as well as lunar basalts have significantly lower Rb/Sr ratios. Instead, the Rb/Sr ratio of the Zagami source region is similar to the composition of terrestrial continental reservoirs (e.g., Newsom, 1995). Thus, the Rb-Sr isotopic systematics of Zagami suggest that it is derived from a highly evolved source region.

4.2. Sm-Nd Isochron

Samarium-neodymium isotopic analyses were also completed on the whole rocks, mineral fractions, and L2 leachates. A Sm-Nd isochron plot of the Zagami fractions is presented in Figure 3 and yields a crystallization age of 166 ± 12 Ma and an initial Nd isotopic composition of $\varepsilon_{Nd}^{143} = -7.23 \pm 0.17$ (MSWD = 3.7). The Sm-Nd age is defined by all of the fractions with the exception of Wr 2 (L2) and Mask 1 (L2) and is concordant with the Rb-Sr age. Unfortunately, the Mask 1 (R) fraction failed to run, making a direct comparison with the Rb-Sr age defined by the purest mineral fractions Mask 1 (R), Mg-Px (R), and Fe-Px (R) impossible. The fact that several of the leachates lie on the Sm-Nd isochron but off the Rb-Sr isochron is typical of how the Rb-Sr and Sm-Nd isotopic systematics of shergottites respond to alteration. The Sm-Nd systematics of the leachates that lie on the isochron are most likely dominated by Nd derived from igneous phosphates known to be present in Zagami (Wadhwa et al., 1994). In contrast, leachates that lie below the isochron are most likely dominated by alteration products. Alteration agents such as water, and alteration products such as calcite and Ca-sulfate, are characterized by low REE abundances, but have elevated Sr abundances. Thus, alteration may affect the Sr isotopic systematics more dramatically than the Nd isotopic systematics. Nevertheless, the fact that some leachates have Nd isotopic compositions that lie significantly below the isochron suggests that

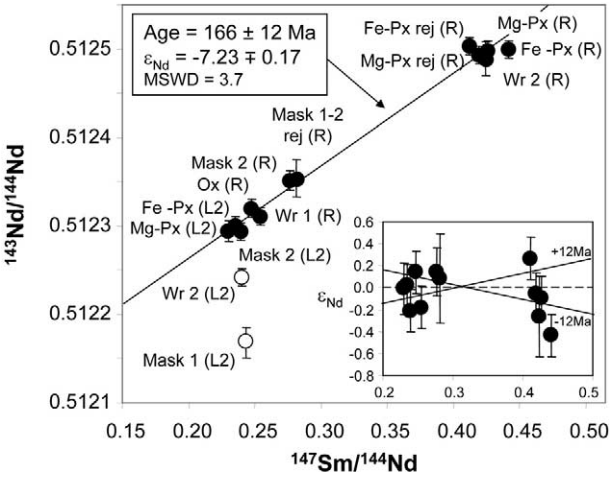

Fig. 3. Sm-Nd isochron plot of Zagami whole-rock, mineral, and leachate fractions. The best age is defined by all silicate and most leachate fractions (filled circles) with the exception of the Mask 1 (L2) and Wr 2 (L2) (open circles). This isochron yields an age of 166 ± 12 Ma and an initial ε_{Nd} value of −7.23 ± 0.17 (MSWD = 3.7). Inset represents deviation of individual fractions from the isochron, in epsilon units.

alteration resulted in the addition of unradiogenic Nd. Although this Nd could be of either terrestrial or martian origin, it is difficult to imagine how terrestrial Nd could have been added to this meteorite given that it is a fall. If this scenario is correct, it implies that the martian surface contains a component characterized by $\varepsilon_{Nd} < -7$ and $^{87}Sr/^{86}Sr$ ratio <0.721, and is therefore isotopically similar to terrestrial crustal sources (e.g., Goldstein and Jacobsen, 1988; Ben Othman, 1989).

The Sm-Nd age determined in this study is concordant with the Sm-Nd age defined for Zagami by Nyquist et al. (1995). However, the isochron defined by the data presented here demonstrates less scatter and results in a more precise age determination. For example, the best Sm-Nd age determined by Nyquist et al. (1995) is 180 ± 37 Ma and uses mineral fractions from both the coarse and fine grained lithologies. Several mineral fractions analyzed by Nyquist et al. (1995) from both the coarse and fine-grained lithologies fall significantly off the Sm-Nd isochron presented here. This may reflect uncertainties associated with analysis of relatively small amounts of Nd, or the presence of a component in Nyquist's chip that was not present in our chip.

The negative initial ε_{Nd}^{143} value of −7.23 ± 0.17 indicates that Zagami is derived from a source region with a long-term LREE enrichment. This source region has an inferred $^{147}Sm/^{144}Nd$ ratio of 0.184, assuming it formed at 4.52 Ga (Borg et al., 2003; Borg and Drake, 2005; Foley et al., 2005) from an initially chondritic reservoir. The source region for Zagami has Sm/Nd ratios that are very similar to the source region for Shergotty ($^{147}Sm/^{144}Nd$ = 0.182) and Los Angeles ($^{147}Sm/^{144}Nd$ = 0.186). Therefore, the source region of Zagami is characterized by Sm/Nd and Rb/Sr ratios that are typical of the most incompatible element-enriched martian source regions.

5. U-PB ISOTOPIC SYSTEMATICS

5.1. U-Pb Isochrons

Uranium-lead isotopic analyses have been completed on the same whole-rock, mineral, and reject fractions, as well as L2 leachates that Rb-Sr and Sm-Nd isotopic analyses have been completed on. The 0.5 M acetic acid whole-rock leachate, Wr 1 (L1), was also analyzed for U-Pb. The U-Pb isochrons are presented in Figure 4a,b. As demonstrated below, the U-Pb isotopic compositions of Zagami are highly disturbed. Therefore, the goal of the U-Pb analyses is not to define the crystallization age of the sample; this is defined by the Rb-Sr and Sm-Nd isochrons. Instead, the U-Pb isotopic systematics of martian samples are used in the context of the Rb-Sr and Sm-Nd ages to constrain the behavior of U and Pb on Mars. As a consequence, the most reliable U-Pb data are those defined by mineral fractions which yield isochron ages that are concordant with Rb-Sr and Sm-Nd isochron ages.

The best ^{238}U-^{206}Pb age and initial $^{206}Pb/^{204}Pb$ isotopic ratio is defined by the purest mineral fractions, which include Mask 1 (R), Mg-Px (R), and Fe-Px (R). This isochron yields an age of 156 ± 6 Ma and an initial $^{206}Pb/^{204}Pb$ ratio of 13.268 ± 0.018 (MSWD = 1.3). This age is younger than the Rb-Sr age determined on the same fractions (176 ± 2 Ma), but concordant with the preferred Rb-Sr (166 ± 6 Ma) and Sm-Nd (166 ± 12 Ma) ages defined by all silicate and oxide mineral fractions. Although this is the most precise U-Pb age that can be determined from our data, an isochron defined by all of the silicate mineral fractions except the Mg-Px rej (R) fraction yields an age of 159 ± 14 Ma and an initial $^{206}Pb/^{204}Pb$ ratio of 13.238 ± 0.090, indicating that to a first order, the ^{238}U-^{206}Pb isotopic systematics of Zagami reflect isotopic growth in an ~166 Ma sample.

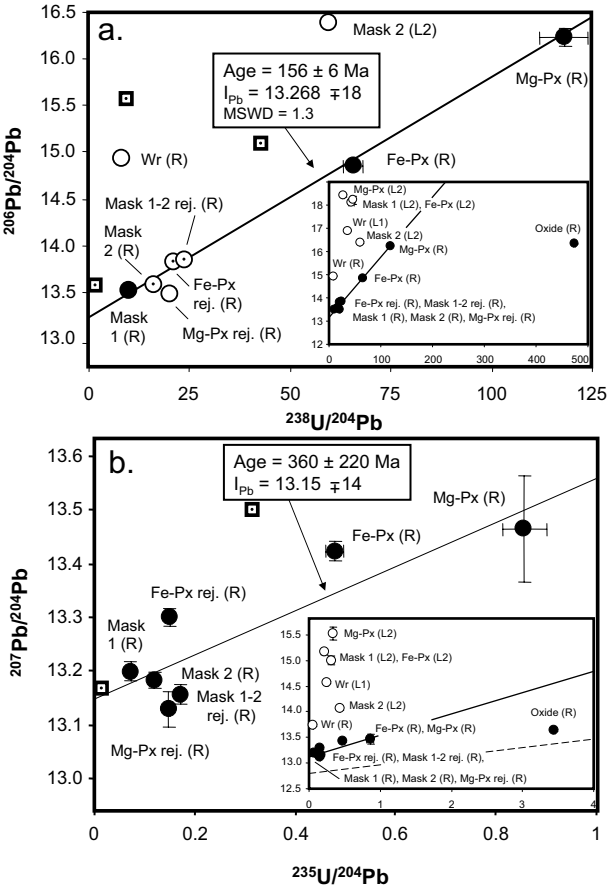

Fig. 4. U-Pb isochron plots of Zagami whole-rock, mineral, and leachate fractions. (a) ^{238}U-^{206}Pb isochron plot. An age of 156 ± 6 Ma and an initial $^{206}Pb/^{204}Pb$ ratio of 13.268 ± 0.018 is defined by mineral fraction residues (filled circles) Mask 1 (R), Fe-Px (R), and Mg-Px (R), and yields a MSWD of 1.3. All silicate fractions except Mg-Px rej (R) define an age of 159 ± 14 Ma (filled circles and open circles with dot). All open circles are Wr (R) and leachates analyzed in this study, whereas squares with dots represent whole rocks and leachates analyzed by Chen and Wasserburg (1986a). (b) ^{235}U-^{207}Pb isochron plot yields no age information. The most precise age of 360 ± 220 Ma and an initial $^{207}Pb/^{204}Pb$ ratio of 13.15 ± 0.14 are defined by all of the silicate mineral fractions (filled circles). Symbols same as in Figure 4a. Dashed line in inset represents 166 Ma reference line with initial $^{207}Pb/^{204}Pb$ = 12.81 (see text).

The concordance between the ^{238}U-^{206}Pb, Rb-Sr, and Sm-Nd ages demonstrates that the ^{238}U-^{206}Pb isotopic systematics of the most pure silicate mineral fractions at least partially reflect the crystallization age of Zagami. The concordance of ages further suggests that, unlike the leaching preformed by Misawa et al. (1997) on mineral fractions from the lherzolitic shergottite Y793605, the leaching of the Zagami mineral fractions has not resulted in significant fractionation of U from Pb in the silicate mineral fractions. This most likely reflects the fact that leaching performed for this study was completed using

weak acids at room temperature for a relatively short period of time. Gaffney et al. (2005) reached the same conclusion regarding leached mineral fractions from uncontaminated Apollo 11 basalt 10017. These authors demonstrated that leachate-residue fractions lie on the same U-Pb isochron, that recombined leachate-residue pairs define the same age and initial Pb isotopic composition as the residue fractions, and that the ^{238}U-^{206}Pb age agrees with Rb-Sr and Sm-Nd ages determined on the same fractions.

The oxide mineral fraction as well as the leachate L1 and L2 fractions do not lie near the ~156 Ma isochron, however. The Ox (R) mineral fraction lies to the right of the isochron, possibly due to Pb removal by the light leaching in 0.5 M acetic acid, which would raise the ^{238}U/^{204}Pb ratio (μ value) of the mineral fraction. This explanation has been invoked to account for apparently high μ values observed in leached oxide-rich mineral fractions from Apollo basalt 15085 (Unruh and Tatsumoto, 1977). If this scenario is correct, ~75% of the Pb must be removed from the oxide mineral fraction by leaching. A more likely explanation for the high μ values of the Ox (R) fraction is that the oxides may not retain Pb efficiently during impact metamorphism. In either case, the Ox (R) mineral fraction appears to have lost Pb relatively recently.

The U-Pb isotopic systematics of the leachate fractions, like the Rb-Sr isotopic systematics, appear to contain a contaminant that is not in isotopic equilibrium with the silicate fractions. This contaminant is characterized by a more radiogenic Pb isotopic composition than the mineral fractions, suggesting that it is derived from a source region with a greater long-term U/Pb ratio than the Zagami source region. Although it is not impossible, it seems unlikely that surface contaminates on Mars will be derived from sources with higher, more fractionated U/Pb ratios than the Zagami source because the Zagami source is one of the most fractionated. We therefore speculate that the Pb contamination is of terrestrial origin and was, perhaps, added to the sample during sawing of the initial meteorite. This is supported by the Pb isotopic compositions of the leachates that approach, or are identical to, terrestrial common Pb values (Table 3). The Rb-Sr, Sm-Nd, and U-Pb isotopic compositions of the leachates suggest that the Sr and Nd contamination could be derived from Mars, whereas the Pb contamination is derived from Earth. This requires the terrestrial contaminant to have relatively high Pb, but low Sr and Nd abundances, whereas the opposite is required for the martian contaminant. Alternatively, all of the Sr, Nd, and Pb contamination observed in the leachates could be derived from Earth.

The ^{235}U-^{207}Pb isochron plot is presented in Figure 4b. Although this plot yields no age information, a line corresponding to an age of 312 ± 1300 Ma and an initial ^{207}Pb/^{204}Pb ratio of 13.20 ± 0.89 is defined by Mask 1 (R), Fe-Px (R), and Mg-Px (R), the purest mineral fractions. A more restricted reference age of 360 ± 220 Ma with an initial ^{207}Pb/^{204}Pb ratio of 13.15 ± 0.14 is defined if all of the silicate mineral fractions are included in the calculation. The large amount of uncertainty in the ^{235}U-^{207}Pb age compared to the ^{238}U-^{206}Pb age is not unexpected, because a small amount of Pb contamination will have a large effect on the limited abundance of radiogenic ^{207}Pb produced by the small proportion of ^{235}U present (<1% ^{238}U) in the rock when it formed. Like the ^{238}U-^{206}Pb system, the leachates lie above the isochron, reflecting the presence of terrestrial contamination, whereas the oxide fraction lies to the right of the isochron most likely reflecting Pb loss.

Previously, Chen and Wasserburg (1986a) reported U-Pb isotopic analyses on a whole rock and two leachates of Zagami. Although an "isochron" defined by the residue, leachate, and calculated total (recombined residue plus leachates) yields a ^{238}U-^{206}Pb age of 231 ± 3 Ma, the similarity to the Rb-Sr, Sm-Nd, and ^{238}U-^{206}Pb crystallization ages that have been determined here, and previously (Shih et al., 1982; Nyquist et al., 1995), appears to be fortuitous. This is because the samples analyzed by Chen and Wasserburg (1986a) have somewhat more radiogenic Pb than the samples that define the 156 Ma ^{238}U-^{206}Pb age in this study (Fig. 4a). Thus, the fractions analyzed by Chen and Wasserburg (1986a) appear to contain some of the radiogenic Pb contaminant that is present in our leachates. Note that the leachates of Chen and Wasserburg (1986a) are less radiogenic than the leachates presented here, implying that they contain less contamination. As a result, the whole-rock residue of Chen and Wasserburg (1986a) could contain a greater proportion of terrestrial contamination than the residues analyzed in this study.

The initial ^{206}Pb/^{204}Pb and ^{207}Pb/^{204}Pb isotopic ratios determined from the isochrons (Fig. 4a,b) indicate that Zagami was derived from a source region with a fairly low μ value. An initial ^{206}Pb/^{204}Pb ratio of 13.268 ± 0.018 corresponds to a source region with a μ value of 3.96 ± 0.02, assuming growth in a reservoir that formed at 4.558 Ga with the initial Pb isotopic composition of the Canyon Diablo meteorite (^{206}Pb/^{204}Pb = 9.307; Tatsumoto et al., 1973; Chen and Wasserburg, 1983). Although there is significantly more uncertainty associated with the initial ^{207}Pb/^{204}Pb ratio (as a result of the poorly defined isochron), the most precise μ value calculated from an initial ^{207}Pb/^{204}Pb ratio of 13.15 ± 0.14 is 4.49 ± 0.22 (using the initial ^{207}Pb/^{204}Pb ratio of the Canyon Diablo meteorite of 10.294; Tatsumoto et al., 1973; Chen and Wasserburg, 1983).

The observations that the only way to obtain a ^{238}U-^{206}Pb isochron age that is concordant with the Rb-Sr and Sm-Nd crystallization ages is to select the purest mineral fractions, and that the ^{235}U-^{207}Pb system yields no coherent linear regression indicates that the U-Pb systematics of Zagami are disturbed. Whereas the purest mineral fractions yield a ^{238}U-^{206}Pb age that is concordant with the Rb-Sr and Sm-Nd ages, the ^{235}U-^{207}Pb system demonstrates significantly more scatter. If both systems were disturbed to the same degree, similar amounts of scatter are expected on both plots, resulting in significantly greater uncertainty associated with the ^{235}U-^{207}Pb age because of the low modern production rate of ^{207}Pb. Furthermore, the μ value calculated for the Zagami source region using the initial ^{207}Pb/^{204}Pb ratio is higher than the μ value calculated from the initial ^{206}Pb/^{204}Pb ratio. In fact, the initial ^{207}Pb/^{204}Pb ratio of Zagami predicted on the basis of the measured initial ^{206}Pb/^{204}Pb ratio is 12.81 (inset Fig. 4b), differing from the best value of 13.15 ± 0.14 determined from the ^{235}U-^{207}Pb isochron. Consequently, all of the mineral fractions lie above a 156 Ma isochron with an initial ^{207}Pb/^{204}Pb ratio of 12.81 in Figure 4b (inset). These observations indicate that the disturbance in the U-Pb system is most clearly manifest in the ^{235}U-^{207}Pb isotopic systematics.

5.2. Disturbances of the U-Pb Isotopic System

To interpret the disturbed U-Pb isotopic systematics of Zagami, it is necessary to discuss idealized Pb growth in an undisturbed martian system. Gale (1972) and Gale and Mussett (1973) have pointed out that undisturbed geologic systems that have experienced lead growth in two stages yield linear arrays on Pb-Pb, U-Pb concordia, and U-Pb isochron plots. Although the Rb-Sr and Sm-Nd isotopic systematics of the basaltic martian meteorites indicate that their source evolved in two stages, isotopic growth in the rocks derived from these sources once they crystallized represents a third stage of evolution. Thus, stage one represents growth in an undifferentiated primordial reservoir; stage two represents growth in a differentiated reservoir presumably produced in association with core, mantle, and crust formation; and a third stage represents isotopic growth in the rocks and minerals derived from the melting of reservoir two. Gale (1972) and Gale and Mussett (1973) also note that three-stage Pb growth forms linear arrays on these U-Pb diagrams under specific circumstances. One case is when the time interval between stages is of limited duration. As noted above, $\varepsilon_{Nd}^{143} - \varepsilon_{Nd}^{142}$ systematics of the martian meteorite suite are consistent with silicate differentiation occurring ~30 Ma after planetary formation. This represents the latest time that U and Pb are likely to be fractionated from their primordial ratio in the martian meteorite source regions. The ~30 Ma time span between planet formation and silicate differentiation will have negligible effect on the growth of radiogenic Pb. Consequently, U-Pb isotopic evolution of mineral fractions derived from martian basalts, such as Zagami, is expected to approximate two stages of growth. The first stage is from the time of silicate differentiation (~4.52 Ga) to source melting and melt crystallization (~166 Ma), and the second is from 166 Ma to present.

5.2.1. *Concordia diagram*

A concordia diagram in which radiogenic Pb is calculated by subtracting primordial Pb composition is presented in Fig. 5. The discordia presented on this diagram is defined by all of the whole-rock, mineral, and leachate fractions and yields a discordia that intercepts concordia at 4584 ± 100 Ma and 70 ± 160 Ma. In a two-stage Pb evolution model, the upper intercept reflects the time in the history of the planet when it had a primordial lead isotopic composition (Gale, 1972). There is no way to equate this age with any evolutionary phase in the planet's history (Gale and Mussett, 1973). In a two-stage model of Pb evolution, the lower intercept represents the time when U and Pb were first fractionated from a primordial reservoir. In a two-stage Pb evolutionary model for a basalt, this represents the crystallization age of the sample.

The scatter of data points on the U-Pb isochron plots presented in Figure 4a,b clearly indicate that the U-Pb system has been disturbed, most likely through the addition of Pb. As a consequence, models in which terrestrial Pb ($^{206}Pb/^{204}Pb$ = 18.2, $^{207}Pb/^{204}Pb$ = 15.5) and martian Pb ($^{206}Pb/^{204}Pb$ = 13, $^{207}Pb/^{204}Pb$ = 14) is mixed with the Wr (R) fraction are plotted on Figure 5. These mixing models demonstrate that contamination of individual fractions by extraneous Pb raises their $^{207}Pb^*/^{235}U$ and $^{206}Pb^*/^{238}U$ ratios along a line that approximates the discordia defined by the mineral, whole-rock and leachate fractions. As a result, it is probable that the U-Pb isotopic systematics displayed on the concordia diagram represent the combined effects of Pb contamination and more or less two stages of Pb growth. It is not possible, therefore, to unambiguously interpret the lower (or upper) discordia intercepts in the context of geochronology.

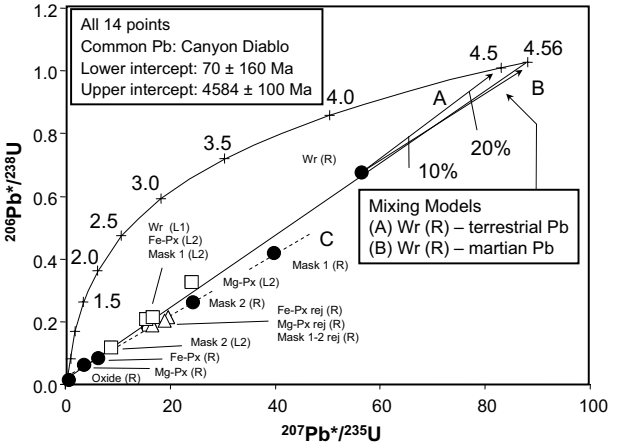

Fig. 5. Concordia plot of Zagami whole-rock, mineral, and leachate fractions. Radiogenic Pb (Pb*) is calculated using primordial Pb value of Tatsumoto et al. (1973). A discordia with a lower intercept of 70 ± 160 Ma and an upper intercept of 4584 ± 100 Ma is defined by all analyzed fractions. In a two-stage model of Pb growth (as suggested for basaltic martian samples by their $\varepsilon_{Nd}^{143} - \varepsilon_{Nd}^{142}$ systematics, see text) the lower intercept reflects the crystallization age of Zagami (Gale, 1972; Gale and Mussett, 1973). However, whole-rock contaminant mixing models (arrows with percent contaminant) demonstrate that Pb contamination of individual mineral fractions results in increased scatter and displacement of points along this discordia. Terrestrial contamination drives fractions above discordia (curve A), whereas a potential martian contaminant characterized by a high $^{207}Pb/^{206}Pb$ ratio drives fractions below discordia (curve B). Thus, the position of individual fractions along discordia reflect a combination of approximately two stages of Pb growth and contamination. A discordia defined by impact glass-rich mineral fractions (dashed line C) has an upper intercept of 4750 Ma and a lower intercept of 116 Ma consistent with the presence of a martian contaminant in these fractions that is characterized by a high $^{207}Pb/^{206}Pb$ ratio. (Note that the amount of Pb contamination required to shift the whole rock a given distance on this diagram represents a near maximum value because the Wr (R) fraction used in the mixing models has the second highest Pb concentration of any analyzed fraction.) The lower intercept does not define but is consistent with the crystallization age of the sample.

The mixing models demonstrate that relatively large amounts of contamination are required before individual points move significantly along the discordia (Fig. 5). The addition of terrestrial contamination moves individual fractions slightly above the discordia defined in Figure 5, whereas addition of martian Pb, characterized by a higher $^{207}Pb/^{206}Pb$ ratio, drives the fractions slightly below the discordia. Interestingly, the fractions that lie below the discordia are those that would be most disturbed by impact processes, that is, those fractions that contain impact-produced glasses (maskelynite and reject mineral fractions). The lower intercept of a line regressed through these glass-rich fractions also intercepts concordia near the crystallization age of Zagami (116 Ma), indicating that even these partially contaminated mineral fractions retain some vestige of the crystallization age of the sample. The upper intercept lies to the right of the concordia curve (4750 Ma), suggesting

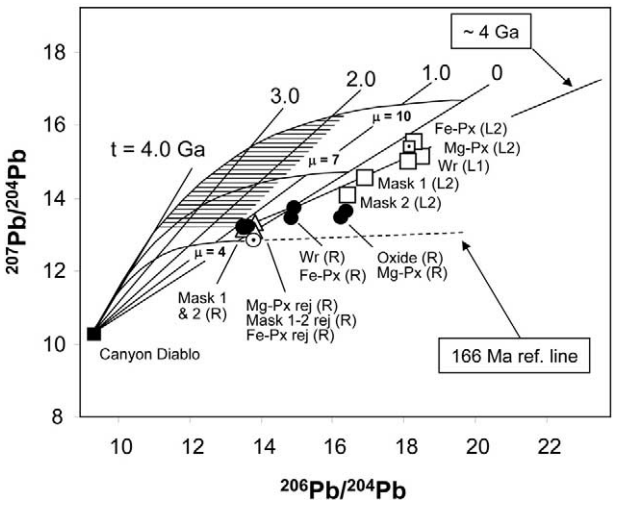

Fig. 6. Pb-Pb isochron plot for Zagami whole-rock and mineral fractions (solid circles), leachates (open squares), and reject fractions (triangles). Curved lines represent single-stage Pb growth models for hypothetical reservoirs with variable μ values. Note that the Zagami residue fractions are shifted above the 166 Ma reference line as a result of contamination. The leachates lie on a line with a slope corresponding to an age of ~4 Ga. Common terrestrial Pb (open square with dot) and initial Zagami Pb defined from U-Pb isochrons (open circle with dot) also lie along this line, suggesting that the leachates are mixtures of these end members. The shaded area represents Pb with isotopic characteristics estimated for martian contaminant. This Pb must be separated from a reservoir that underwent a single stage of growth before ~1.8 Ga (see text).

that the contaminant present in the impact melt glasses is characterized by an elevated $^{207}Pb/^{206}Pb$ ratio (mixing model B, Fig. 5). In contrast to the impact glass-rich fractions, the leachates tend to lie above the discordia in Figure 5, consistent with the presence of Pb with an isotopic composition that is more similar to terrestrial Pb (mixing model A, Fig. 5).

5.2.2. ^{206}Pb-^{207}Pb isochron diagram

The relatively large amount of disturbance observed in the ^{235}U-^{207}Pb system compared to the ^{238}U-^{206}Pb system is also illustrated on the $^{206}Pb/^{204}Pb$-$^{207}Pb/^{204}Pb$ isochron plot (Fig. 6). If the Pb isotopic systematics were not disturbed, and Pb growth occurred in two stages, the mineral fractions are expected to lie on a line with a slope corresponding to an age of ~166 Ma. Furthermore, since isotopic growth of martian meteorite sources is approximated by two stages of growth, this ideal isochron should intersect a single-stage growth curve of primordial Pb with a μ value near 4 (the μ value calculated on the basis of the initial $^{206}Pb/^{204}Pb$ ratio). Note, however, that all of these mineral fractions are shifted to higher $^{207}Pb/^{204}Pb$ ratios above the 166 Ma reference line. Again, this suggests that the $^{207}Pb/^{206}Pb$ ratio of the mineral fractions is higher than expected if the U-Pb isotopic system was undisturbed. In contrast to the mineral fractions, the leachates analyzed in this study as well as those from Chen and Wasserburg (1986a) fall along a line in Figure 6 with a slope corresponding to an age of ~4 Ga. The fact that both terrestrial common Pb and the initial Pb isotopic composition of Zagami determined from the U-Pb isochrons lie along this line further suggests that the leachates are mixtures of Pb that is derived from leachable igneous sources, presumably phosphates, and Pb derived from terrestrial contamination.

The U-Pb isotopic disturbances observed in Zagami are typical of disturbances observed in the U-Pb isotopic systematics of other basaltic martian meteorites. Although U-Pb isotopic analyses have been completed on several whole rocks and leachates of basaltic meteorites (EETA79001, ALH77005, LEW88516, Zagami) by Chen and Wasserburg (1986a, 1986b), analyses of mineral separates have only been completed on Shergotty and Y793605 (Chen and Wasserburg, 1986a; Misawa et al., 1997). Nevertheless, all of the samples analyzed so far demonstrate U-Pb isotopic disturbances that are similar to those discussed above for Zagami. Thus, the ^{207}Pb-^{206}Pb (and ^{235}U-^{207}Pb) ages of these samples are significantly older than their Rb-Sr, Sm-Nd, and ^{238}U-^{206}Pb ages. Furthermore, the ^{238}U-^{206}Pb ages are also often disturbed (Chen and Wasserburg, 1986a; Misawa et al., 1997). It is therefore probable that the U-Pb isotopic systematics of all of the basaltic shergottites have been disturbed by the same mechanism.

5.3. Mechanisms to Disturb the U-Pb Isotopic Systematics of the Shergottites

5.3.1. Pb isotopic composition of the contaminants

The U-Pb isotopic data discussed above demonstrate that there are at least two contaminants present in Zagami. The first is easily removed by leaching and appears to have the isotopic composition of terrestrial common Pb. As argued above, this contaminant was probably added to the sample during handling, curation, or sawing. The second contaminant appears to be present in the silicate mineral fraction residues and is characterized by a relatively high $^{207}Pb/^{206}Pb$ ratio. This contaminant is physically associated with the mineral fractions that are most disturbed by impact processes, that is, those containing significant amounts of impact melt (the maskelynite and reject fractions). This suggests that this contaminant is present in the impact melt glasses and has been added to them through the shock process. Rao et al. (1999) demonstrated that elevated sulfur abundances in impact glass from EET79001 was likely to reflect the presence of martian soil added to these glasses during impact. Therefore, the fact that the reject mineral fractions containing relatively large proportions of impact melt glass have the highest $^{207}Pb/^{206}Pb$ ratios suggests that the contaminant present in the Zagami mineral fractions may ultimately be derived from martian surface material.

The Pb isotopic composition of this contaminant cannot be tightly constrained from the Zagami U-Pb isotopic data. However, several reject mineral fractions that lie off the U-Pb and Pb-Pb isochrons have elevated $^{207}Pb/^{206}Pb$ ratios up to 0.98 (Table 3), indicating that the $^{207}Pb/^{206}Pb$ ratio of the contaminant must be at least 1. The contaminant must also have a $^{207}Pb/^{204}Pb$ ratio that is in excess of 13.15, the initial $^{207}Pb/^{204}Pb$ ratio determined from the isochron. This is because the best-measured initial $^{207}Pb/^{204}Pb$ ratio is higher than the value predicted on the basis of the minimally disturbed ^{238}U-^{206}Pb isochron. Thus, the $^{207}Pb/^{204}Pb$ ratio of the contaminant must have a Pb isotopic composition that, when added to the mete-

orite, results in higher $^{207}Pb/^{204}Pb$ ratios of the mineral fractions.

5.3.2. *Mechanisms to produce a contaminant with an elevated $^{207}Pb/^{206}Pb$ ratio*

Modern Pb with a $^{207}Pb/^{206}Pb$ ratio of ≥ 1 and a $^{207}Pb/^{204}Pb$ ratio of ≥ 13.15 cannot be produced by a single stage of growth in a reservoir with a constant μ value since 4.56 Ga. Instead, at least two stages of growth are required in reservoirs with differing μ values. The first stage of growth must occur in a reservoir with a relatively high μ value to produce an enrichment of ^{207}Pb relative to ^{206}Pb. Continued decay of U in this reservoir will lower its $^{207}Pb/^{206}Pb$ ratio because its $^{238}U/^{235}U$ ratio is increasing through time. Thus, to preserve high $^{207}Pb/^{206}Pb$ ratios in martian materials until the present, Pb must be fractionated from U early in the evolutionary history of the system.

The timing of this fractionation event can be partially constrained. The shaded area in Figure 6 represents single-stage Pb that has a $^{207}Pb/^{206}Pb$ ratio greater than 1, and $^{207}Pb/^{204}Pb$ ratio that is greater than 13.15. Lead removed from a reservoir that formed at 4.56 Ga with a μ value greater than ~5 (before ~1.8 Ga ago) will satisfy the minimum isotopic criteria of the contaminant. This scenario requires U and Pb to be fractionated completely, that is, formation of a second reservoir with a μ value of 0. The extreme U-Pb fractionation required by this scenario ultimately suggests that this is a minimum age and that U-Pb fractionation likely occurred before 1.8 Ga.

Igneous processes involving pyroxene and olivine cannot strongly fractionate U from Pb. However, U is significantly more mobile than Pb in some fluid-dominated weathering conditions. Asmerom and Jacobsen (1993) demonstrated that U is removed in preference to Pb in modern terrestrial weathering environments as a result of the increased solubility of U relative to Pb. In fact, they found that the μ values of crustal weathering residues could be lowered from their original values by a factor of ~2. If the low U/Pb of the source of the Zagami contaminant reflects U removal by weathering, a U-rich surface material is expected to be present in Mars. Alternatively, chemical precipitates formed from aqueous solutions may have low U/Pb ratios as a result of a greater compatibly of Pb compared to U in these precipitates. Martian surface materials such as soils could therefore represent material from which U was removed, and/or Pb concentrated, by water. Thus, it is possible that fluid-based weathering of surface materials occurring before 1.8 Ga could strongly fractionate U/Pb ratios, accounting for the Pb isotopic systematics of the contaminant. If this material is present in the impact melt glasses in Zagami, as suggested for EETA79001 by Rao et al. (1999), it could explain the U-Pb isotopic disturbances observed in the Zagami mineral fractions. Production of the Pb isotopic systematics of the contaminant by fluid-based weathering processes is consistent with a soil origin for the contaminant. If the contaminant Pb observed in the martian meteorites is derived from the soils, then the soils are likely to have been geochemically altered by ancient fluid-based weathering processes.

5.4. $^{238}U/^{204}Pb$ Ratio of Planetary Reservoirs

5.4.1. *Comparison of reservoirs from Earth, the Moon, and Mars*

Estimations of the μ value of planetary mantle and crustal reservoirs on Earth, the Moon, and Mars are constrained to varying degrees on each body. Because U and Pb are not strongly fractionated by igneous processes, the μ values of these reservoirs in turn constrain the μ values of the bulk planet. For example, the μ values of the Earth's mantle and crust are estimated to be 8 to 10 and 11 to 12, respectively (e.g., Zartman and Haines, 1988; Asmerom and Jacobsen, 1993), suggesting that bulk silicate Earth has a μ value of 10 ± 2. In contrast to terrestrial samples, the ancient age and impact metamorphosed nature of many lunar samples, combined with their very low Pb abundances, has resulted in much more uncertain estimations of μ values of lunar sources (e.g., Tera and Wasserburg, 1972; Tera and Wasserburg, 1974; Tera et al., 1974). Nyquist and Shih (1992) noted that the μ values estimated for mare basalt source regions ranged from ~0 to 650, with most estimates between 100 and 400. Unruh and Tatsumoto (1977) argued that the μ values for mare source regions should be representative of the bulk Moon, concluding that the bulk Moon has a μ value between 100 and 300. Finally, the μ value for the Zagami source is estimated to be 3.96 ± 0.02. This is the only internally consistent estimate of the $^{238}U/^{204}Pb$ of any martian source. The Rb-Sr, Sm-Nd, and Lu-Hf (Blichert-Toft et al., 1999) isotopic systematics of Zagami indicate that it is derived from one of the most highly fractionated and evolved reservoirs on any sampled differentiated body (Borg et al., 2003), suggesting that the μ value of the Zagami source is likely to represent a near maximum value for any martian mantle or crustal reservoir.

Despite the uncertainties, it is evident that the μ value for bulk Moon is greater than the μ value for bulk Earth, which is in turn greater than the μ value for bulk Mars. This could reflect differences in U/Pb ratios of the bulk planet, or removal of Pb from the silicate portion of the body by core formation. Chen and Wasserburg (1986a) noted that the U-Pb isotopic systematics of martian meteorites indicated derivation from low μ sources and speculated that this was consistent with higher volatile element (e.g., K, Rb, and Pb) abundances for Mars (Dreibus and Wänke, 1985). This is also supported by the observation that the bulk $^{87}Rb/^{86}Sr$ ratios of the Moon (0.042; Ranen and Jacobsen, 2005), Earth (0.083), and Mars (0.16; Borg et al., 1997) inversely correlate with estimates of their bulk μ values. Because Rb is not fractionated from Sr by core formation, this inverse correlation suggests that that variations of U/Pb ratios in the silicate portions of the Moon, Earth, and Mars reflect variations in the volatile element budgets of these bodies.

5.4.2. *U/Pb ratios of martian meteorite source regions*

It is difficult to estimate the μ value of the source regions of the basaltic martian meteorites other than Zagami because their U-Pb isotopic systematics are clearly disturbed. Some of the meteorites, however, yield ^{238}U-^{206}Pb ages that are concordant with their Rb-Sr and Sm-Nd ages (Chen and Wasserburg, 1986a; Chen and Wasserburg, 1986 b; Fig. 7) and are therefore

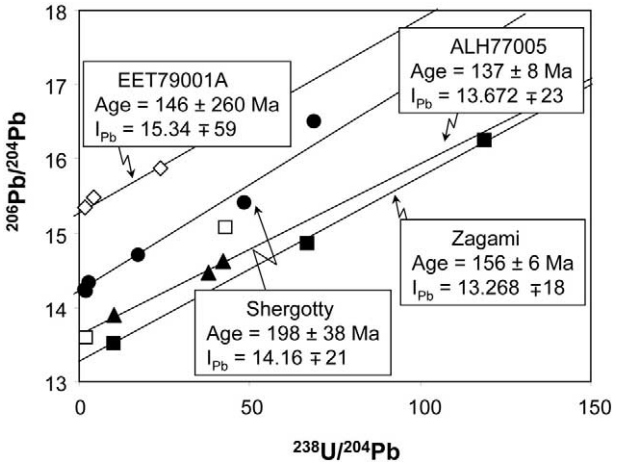

Fig. 7. ^{238}U-^{206}Pb isochron plot of basaltic meteorites which yield ages that are roughly concordant with their Rb-Sr and/or Sm-Nd ages (i.e., ~170 Ma). The U-Pb isotopic systematics of these samples appear to be the least affected by impact metamorphism and alteration. EETA79001A (open diamonds), ALH77005 (filled triangles), Zagami (open squares) are leachate whole-rock tie lines, whereas Shergotty (filled circles) are whole-rock, mineral, and leachate data (Chen and Wasserburg, 1986a; Chen and Wasserburg, 1986b). Filled squares are Zagami mineral fraction residues from this study. There is no correlation between the initial $^{206}Pb/^{204}Pb$ (I_{Pb}) determined from these isochrons and initial Sr and Nd, suggesting that the initial $^{206}Pb/^{204}Pb$ ratios determined from leachate whole-rock tie lines are not reliable despite yielding appropriate crystallization ages.

likely to have the least disturbed U-Pb isotopic systematics. However, the μ values of the meteorite sources calculated from the initial $^{206}Pb/^{204}Pb$ ratios in Figure 7 do not correlate with Rb/Sr or Sm/Nd ratios calculated for the same sources. This could reflect a difference in the way U-Pb, Rb-Sr, and Sm-Nd are fractionated in the source regions of the meteorites. Borg et al. (1997, 2003) have argued that Rb-Sr and Sm-Nd are fractionated in the meteorite source regions by either crystallization of a magma ocean or by partial melting of an initially solid Mars. The lack of correlation of U/Pb with Rb/Sr and Sm/Nd ratios of the martian basalt source regions could therefore reflect fractionation of U from Pb by a process other than silicate crystallization or melting. The involvement of sulfides, metals, or metasomatic agents could all potentially fractionate U from Pb in a manner that is different from what is predicted for silicate systems.

Alternatively, the μ values estimated from the ^{238}U-^{206}Pb isotopic systematics could be erroneous as a result of disturbance of the U-Pb isotopic systematics of these meteorites. This possibility is supported by the observation that the leachate whole-rock tie-line for Zagami from Chen and Wasserburg (1986a) yields a $^{206}Pb/^{204}Pb$ ratio that is different from the ratio determined from the residue mineral fractions from this study (Fig. 7). Furthermore, note that the basaltic shergottite EET79001A, which is thought to contain a large amount of extraneous material possibly derived from martian soil (Rao et al., 1999), has the most radiogenic initial $^{206}Pb/^{204}Pb$ ratio. This suggests that the most coherent isotopic systematics could be disturbed and therefore unrepresentative of the martian basalt source regions. Additional U-Pb isotopic analyses of mineral fractions from minimally disturbed martian meteorites are probably required before potential variations in the U/Pb ratios of their source regions can be rigorously evaluated.

6. CONCLUSION

The crystallization age of Zagami is well-defined by concordant Rb-Sr, Sm-Nd, and ^{238}U-^{206}Pb ages of 166 ± 6 Ma, 166 ± 12 Ma, and 156 ± 6 Ma, respectively. The concordance of these ages suggests that the ^{238}U-^{206}Pb isotopic system of the most pure mineral fractions has not been significantly disturbed by postcrystallization processes. In contrast, the ^{235}U-^{207}Pb systems demonstrate more disturbance as manifested by discordant or imprecise ages derived from chronometers that incorporate the ^{235}U-^{207}Pb decay series. The isotopic disturbances observed in the silicate and reject mineral fractions are interpreted to be the result of the addition of Pb characterized by an elevated $^{207}Pb/^{206}Pb$ ratio. This Pb must ultimately be derived from an ancient high μ martian source that was subsequently fractionated to a lower μ value before 1.8 Ga. This fractionation of U from Pb early in martian history probably requires aqueous processes to efficiently separate U from Pb, indicating the contaminant could be derived from martian surface material. The initial $^{206}Pb/^{204}Pb$ ratio determined from the ^{238}U-^{206}Pb isochron is 13.268 and corresponds to a source region with a μ value of 3.96. Although this is a maximum value, given the disturbance of the U-Pb isotopic system, it is significantly lower than estimates for terrestrial or lunar sources regions. The initial $^{87}Sr/^{86}Sr$ ratio and ε_{Nd} value of Zagami are 0.721566 ± 0.000082 and −7.23 ± 0.17, respectively, and indicate that this meteorite is derived from one of the most highly evolved martian source regions. It is therefore probable that the μ value estimated for Zagami represents a near maximum martian value. The low μ value of the Zagami source likely reflects the high volatile element content of Mars relative to other terrestrial bodies.

Acknowledgments—Reviews of this work by K. Mezger and two anonymous reviewers were of great use and improved the manuscript. Discussions with J. Connelly are also much appreciated. This work was supported by NASA grant NAG5-11555 to Lars Borg.

Associate editor: R. J. Walker

REFERENCES

Asmerom Y. and Jacobsen S. B. (1993) The Pb isotopic evolution of the earth: Inferences from river water suspended loads. *Earth Planet. Sci. Lett.* **115,** 245–256.

Ben Othman D., White W. M., and Patchett J. (1989) The geochemistry of marine sediments, island arc magma genesis and crust mantle recycling. *Earth Planet. Sci. Lett.* **94,** 1–24.

Blichert-Toft J., Gleason J. D., Télock P., and Albarède F. (1999) The Lu-Hf isotope geochemistry of shergottites and the evolution of the martian mantle-crust system. *Earth Planet. Sci. Lett.* **173,** 25–39.

Borg L. E. and Drake M. J (2005) A review of meteorite evidence for the timing of magmatism and of surface or near-surface liquid water on Mars. *J. Geophys. Res. -Planets.* 110, E12SO3, doi: 10.1029/2005JE002402, 2005.

Borg L. E. and Draper D. A. (2003) A petrogenetic model for the origin and compositional variation of the martian basaltic meteorites. *Meteor. Planet. Sci.* **38,** 1713–1731.

Borg L. E., Nyquist L. E., Wiesmann H., and Shih C.-Y. (1997) Constraints on Martian differentiation processes from Rb-Sr and Sm-Nd isotopic analyses of the basaltic shergottite QUE94201. *Geochim. Cosmochim. Acta* **61,** 4915–4931.

Borg L. E., Connelly J. N., Nyquist L. E., Shih C.-Y., Wiesmann H., and Reese Y. (1999) The age of the carbonates in martian meteorite ALH84001. *Science* **286,** 90–94.

Borg L. E., Nyquist L. E., Reese Y., and Wiesmann H. (2002) Constraints on the petrogenesis of martian meteorites from the partially disturbed Rb-Sr and Sm-Nd isotopic systematics of LEW88516 and ALH77005. *Geochim. Cosmochim. Acta* **66,** 2037–2053.

Borg L. E., Nyquist L. E., Wiesmann H., Shih C.-Y., and Reese Y. (2003) The age of Dar al Gani 476 and the differentiation history of the martian meteorites inferred from their radiogenic isotopic systematics. *Geochim. Cosmochim. Acta* **67,** 3519–3536.

Chen J. H. and Wasserburg G. J. (1983) The least radiogenic Pb in iron meteorites. *Lunar Planet Sci. Conf.* **XIV,** 103–104.

Chen J. H. and Wasserburg G. J. (1986a) Formation ages and evolution of Shergotty and its parent planet from U-Th-Pb systematics. *Geochim. Cosmochim. Acta* **50,** 955–968.

Chen J. H. and Wasserburg G. J. (1986b) S≠N=C. *Lunar Planet Sci. Conf.* **XVIII**, 113–114.

Dreibus G. and Wänke H. (1985) Mars: A volatile-rich planet. *Meteor. Planet. Sci.* **20,** 367–380.

Foley N. C., Wadhwa M., Borg L. E., Janney P. E., Hines R., and Grove T. L. (2005) The early differentiation history of Mars from new constraints on ^{182}W-^{142}Nd isotope systematics in the SNC meteorites. *Geochim. Cosmochim. Acta* **69,** 4557–4571.

Gaffney A., Borg L. E., and Asmerom Y. (2005) ^{238}U-^{206}Pb Age and uranium-lead isotope systematics of mare basalt 10017. *Lunar & Planetary Science Conference* **XXXVI,** abstract 1478 (CD-ROM).

Gale N. H. (1972) Uranium-lead systematics in lunar basalts. *Earth Planet. Sci. Lett.* **17,** 65–78.

Gale N. H. and Mussett A. E. (1973) Episodic uranium-lead models and the interpretation of variations in the isotopic composition of lead in rocks. *Rev. Geophys. Space Phys.* **11,** 37–86.

Goldstein S. J. and Jacobsen S. B. (1988) Nd and Sr isotopic systematics of river water suspended material: Implications for crustal evolution. *Earth Planet. Sci. Lett.* **87,** 249–265.

Harper C. L., Nyquist L. E., Bansal B., Wiesmann H., and Shih C.-Y. (1995) Rapid accretion and early differentiation of Mars indicated by ^{142}Nd/^{144}Nd in SNC meteorites. *Science* **267**, 213–217.

Jones J. H. (1989) Isotopic relationships among the Shergottites, Nakhlites and Chassigny. *Proc. 19th Lunar Planet. Sci. Conf.* 465–47.

Kleine T., Mezger K., Munker C., Palme H., and Bischoff A. (2004) 182Hf-182W isotope systematics of chondrites, eucrites and martian meteorites: Chronology of core formation and early mantle differentiation in Vesta and Mars. *Geochim. Cosmochim. Acta* **68,** 2935–2946.

Lee D.-C. and Halliday A. N. (1997) Rapid accretion and early core formation on asteroids and the terrestrial planets from Hf-W chronometry. *Nature* **418,** 952–955.

Ludwig K. R. (2001) *Users Manual for Isoplot/Ex v. 2.49: A Geochronological Toolkit for Microsoft Excel.* Berkeley Geochronology Center Special Publication No. 1a.

McCoy T. J., Taylor G. J., and Keil K. (1992) Zagami: A product of a two-stage magmatic history. *Geochim. Cosmochim. Acta* **56,** 3571–3582.

Misawa K., Nakamura N., Premo W. R., and Tatsumoto M. (1997) U-Th-Pb isotopic systematics of lherzolitic shergottite Yamato-793605. *Antarct. Meteorite. Res.* **10,** 95–108.

Newsom H. E. (1995) Composition of the solar system, planets, meteorites and major terrestrial reservoirs. In *Global Earth Physics: A Handbook of Physical Constraints* AGU Reference Shelf 1 (ed. T. J. Ahrens), American Geophysical Union, pp. 159–189.

Nyquist L. E., and Shih C. -Y. (1992) The isotopic record of lunar volcanism. *Geochim. Cosmochim. Acta* **56,** 2213–2234.

Nyquist L. E., Wooden J., Bansal B., Wiesmann H., McKay G. A., and Bogard D. D. (1979) Rb-Sr age of Shergotty achondrite and implications for metamorphic resetting of isochron ages. *Geochim. Cosmochim. Acta* **43,** 1057–1074.

Nyquist L. E., Bansal B. M., Wiesmann H., and Shih C.-Y. (1995) "Martians" young and old: Zagami and ALH84001. *Lunar Planet. Sci. Conf.* **XXVI**, 1065–1066 (abstract).

Nyquist L. E., Reese Y. D., Wiesmann H., and Shih C.-Y. (2000) Rubidium-strontium age of Los Angeles shergottite. *Meteor. Planet. Sci.* **35,** A121–A122 (abstract).

Nyquist L. E., Bogard D. D., Shih C-.Y., Greshake A., Stoffler D., and Eugster O. (2001) Ages and geologic histories of the Martian meteorites. In *Chronology and Evolution of Mars, Space Science Review* Vol. 96 (ed. R. Kallenbachetet al.), pp. 105–164, Kluwer Academic Press.

Premo W. R. and Tatsumoto M. (1991) U-Th-Pb isotopic systematics of lunar norite 78235. *Proceed. 21st Lunar Planet. Sci. Conf.* 89–100.

Ranen M. C. and Jacobsen S. B. (2005) Isotopic composition of lunar soils and the early differentiation of the Moon. *Lunar Planet. Sci. Conf.* **XXXVI,** abstract 1274 (CD-ROM).

Rao M. N., Borg L. E., McKay D. S., and Wentworth S. J. (1999) Martian soil component in impact glasses in a martian meteorite. *Geophys. Res. Lett.* **26,** 3265–3268.

Shih C.-Y., Nyquist L. E., Bogard D. D., McKay G. A., Wooden J. L., Bansal B. M., and Wiesmann H. (1982) Chronology and petrogenesis of young achondrites, Shergotty, Zagami and ALHA 77005: Late magmatism on a geologically active planet. *Geochim. Cosmochim. Acta* **46,** 2323–2344.

Stolper E. and McSween H. Y. Jr. (1979) Petrology and origin of the shergottite meteorites. *Geochim. Cosmochim. Acta* **43,** 589–602.

Tatsumoto M., Knight J. K., and Allègre C. J. (1973) Time differences in the formation of meteorites as determined from the ratio of lead-207 to lead-206. *Science* **180,** 1279–1283.

Tera F. and Wasserburg G. J. (1972) U-Th-Pb systematics in three Apollo 14 basalts and the problem of initial Pb in lunar rocks. *Earth Planet. Sci. Lett.* **14,** 281–304.

Tera F. and Wasserburg G. J. (1974) U-Th-Pb systematics on lunar rocks and inferences about lunar evolution and the age of the Moon. *Proc. 5th Lunar Sci. Conf.* 1571–1599.

Tera F., Papanastassiou D. A., and Wasserburg G. J. (1974) Isotopic evidence for a terminal lunar cataclysm. *Earth Planet. Sci. Lett.* **22,** 1–21.

Unruh D. M. and Tatsumoto M. (1977) Evolution of mare basalts: The complexity of the U-Th-Pb system. *Proceed. 8th Lunar Sci. Conf.* 1673–1696.

Wadhwa M., McSween H. Y., and Crozaz G. (1994) Petrogenesis of shergottite meteorites inferred from minor and trace element microdistributions. *Geochim. Cosmochim. Acta* **58,** 4213–4229.

Zartman R. E. and Haines S. M. (1988) The plumbotectonic model for Pb isotopic systematics among major terrestrial reservoirs-A case for bi-directional transport. *Geochim. Cosmochim. Acta* **52,** 1327–1339.